Indian J. pure appl. Math., **27**(11) : 1125-1135, November 1996

THE EFFECT OF INERTIAL SURFACE ON CAPILLARY-GRAVITY WAVES GENERATED BY A MOVING SOURCE

A. K. PRAMANIK AND D. BANIK

Department of Applied Mathematics, Calcutta University, Calcutta-700 054

(*Received* 6 *February* 1995; *after revision* 22 *April* 1996 ; *accepted* 30 *April* 1996)

The linear capillary-gravity waves generated on an inertial surface of a fluid of finite uniform depth, by moving oscillatory surface pressure distribution is considered. The steady far field wave pattern is determined for all values of the parameters and the effect of inertial surface on wave pattern is studied. That the inertial surface has some damping effect is conclusively established. It is found that a particular wave which propagates in non-inertial surface for some values of the parameters may not propagate in the inertial case for the same values of the parameters.

1. INTRODUCTION

In this paper we study the capillary-gravity waves generated by a moving oscillatory pressure distribution acting on the surface of an unbounded fluid of finite depth. The fluid is inviscid, incompressible and is completely covered by an inertial surface composed of a thin uniform distribution of disconnected heavy floating matter. The corresponding problem without inertial surface has been investigated by Pramanik and Majumdar[1]. The various problems with inertial surface has been investigated by a number of authors. Among their works, mention may be made of the works of Peters[2] and Rhodes-Robinson[3]. But no author discussed in detail and explicitly the effect of the inertial surface on the resulting wave pattern. However, in the present problem which has not yet been investigated, this effect is shown in greater detail.

In order to understand the effect we now state briefly the results of the corresponding problem in the non-inertial case i.e., the case when the fluid is not covered by an inertial surface. In this case, the steady state at far field from the source consists, in general, of six progressive waves : four gravity waves and two capillary waves which are characterised by three dimensionless parameters. Supposing ω to be the frequency of oscillation of the moving pressure distribution, V the uniform velocity of the pressure distribution, T' the surface tension, h the uniform depth of the fluid and ρ the volume density of the fluid, the three parameters are

$$a = \omega(h/g)^{1/2}, \quad b = \frac{V}{(gh)^{1/2}}, \quad c = \frac{T}{gh^2}$$

where $T = T'/\rho$. The critical cases which arise due to coalescence of the roots of the frequency equations are represented by some surface $f(a, b, c) = 0$, called the critical surface in the parametric space (a, b, c). In this case it is found that the intersecting curves of the critical surface by the plane c = constant have only two forms. For $0 < c < 1/3$ this intersecting curve divides the whole positive quadrant of the $(a - b)$ plane into five distinct regions, in each of which the set of roots of the frequency equations is different, while for any $c \geq 1/3$ the corresponding curve divides the plane into two such regions.

In the inertial case i.e., the case when the fluid is covered by an inertial surface, the ultimate steady state consists of the same number of progressive waves : four gravity waves and two capillary waves similar to the non-inertial case, however with modified amplitudes and phases. But, besides the parameters a, b, c there exists a new dimensionless parameter, namely $\alpha = \varepsilon/h$ where $\rho\varepsilon$ is the area density of the inertial surface. For the existence of this parameter the frequency curve and critical surface are modified. As before there are two different intersecting curves of the ciritical surface for different ranges of c, α whose complete determination is a different task from the previous case. However, for $0 < c < ((1/3) + \alpha)$ the intersecting curve divides the whole positive quadrant of the $(a - b)$ plane into seven distinct regions and for $c \geq ((1/3) + \alpha)$ the corresponding curve divides the plane into three distinct regions and accordingly the propagation of waves in this case become modified. Specifically, it is found here that the existence of the inertial surface puts some restriction on the propagation of resulting waves. This implies that a particular wave which exists for a certain value of (a, b) in the non-inertial case may not exist in the present case for the same value of (a, b). This will be clear, if we compare the region R_3 for points of which all the waves exist with the corresponding region in the inertial case, in view of the total number of points constituting those regions. In the inertial case the set of points (a, b) constituting that region is smaller in size than that in the non-inertial case.

2. Formulation and Formal Solution

We consider an unbounded fluid of volume density ρ whose surface is completely covered by an inertial surface composed of a thin uniform distribution of disconnected heavy floating matter of area density $\rho\varepsilon$, say. We take x-axis along the undisturbed inertial surface and y-axis vertically upwards. The system being initially at rest, waves are produced by the continued application of the pressure distribution $p(x; t) = f(x)\, e^{i\omega t}$ which at the same time moves along the positive direction of x-axis with unfirom velocity V.

Let $\varphi(x, y; t)$ be the velocity potential, $\eta(x; t)$ the surface elevation and T' the surface tension of the fluid. Then in the co-ordinate system which moves with the velocity V we have the following linearised initial value problem :

$$\frac{\partial^2\varphi}{\partial x^2}+\frac{\partial^2\varphi}{\partial y^2}=0, \quad \text{in } -\infty < x < \infty, \quad -h \le y \le 0, \quad t \ge 0 \qquad \text{... (2.1)}$$

$$\left.\begin{aligned} &\frac{f(x)}{\rho}\, e^{i\omega t}+D\varphi+g\eta+\varepsilon D^2\eta=\frac{T'}{\rho}\frac{\partial^2\eta}{\partial x^2} \qquad \text{... (2.2)} \\ &\text{at} \quad y = 0 \\ &D\eta=\frac{\partial\varphi}{\partial y} \qquad \text{... (2.3)} \end{aligned}\right\}$$

where

$$D = \partial/\partial t - V\frac{\partial}{\partial x}$$

$$\frac{\partial\varphi}{\partial y}=0 \quad \text{at} \quad y = -h \qquad \text{... (2.4)}$$

and

$$\varphi(x, y; 0)=0, \quad \eta(x; 0) = 0. \qquad \text{... (2.5)}$$

The formal solution of the problem is obtained by Fourier-transforming the above system of equations with respect to x and then using the Fourier inversion formula. The following integral representation for η with dimensionless variables can be easily obtained,

$$\eta(x; t)=\frac{1}{2\rho\, gh\sqrt{2\pi}}\sum_{m=1}^{\infty} I_m \qquad \text{... (2.6)}$$

where

$$I_1=\int_0^{\infty} F_1(\lambda)\exp\{i[\lambda x+(\sigma+b\lambda)t]\}\, d\lambda,$$

$$I_2=\int_0^{\infty} F_2(\lambda)\exp\{i[\lambda x-(\sigma-b\lambda)t]\}\, d\lambda,$$

$$I_3=-\int_0^{\infty} F_1(\lambda)\exp\{i(\lambda x+at)\}\, d\lambda$$

$$I_4=-\int_0^{\infty} F_2(\lambda)\exp\{i(\lambda x+at)\}\, d\lambda,$$

$$I_5=\int_0^{\infty} F_3(\lambda)\exp\{-i[\lambda x-(\sigma-b\lambda)t]\}\, d\lambda$$

$$I_6=\int_0^{\infty} F_4(\lambda)\exp\{-i[\lambda x+(\sigma+b\lambda)t]\}\, d\lambda,$$

$$I_7 = -\int_0^\infty F_3(\lambda) \exp\{-i(\lambda x - at)\}\, d\lambda$$

$$I_8 = -\int_0^\infty F_4(\lambda) \exp\{-i(\lambda x - at)\}\, d\lambda$$

and

$$F_1(\lambda) = \frac{\lambda q(\lambda) \tanh\lambda}{(1 + \alpha\lambda \tanh\lambda)(\sigma + b\lambda - a)\sigma},$$

$$F_2(\lambda) = \frac{\lambda q(\lambda) \tanh\lambda}{(1 + \alpha\lambda \tanh\lambda)(\sigma - b\lambda + a)\sigma},$$

$$F_3(\lambda) = \frac{\lambda q(-\lambda) \tanh\lambda}{(1 + \alpha\lambda \tanh\lambda)(\sigma - b\lambda - a)\sigma},$$

$$F_4(\lambda) = \frac{\lambda q(-\lambda) \tanh\lambda}{(1 + \alpha\lambda \tanh\lambda)(\sigma + b\lambda + a)\sigma},$$

$$\sigma = \left[\frac{(\lambda + c\lambda^3)\tanh\lambda}{(1 + \alpha\lambda \tanh\lambda)}\right]^{1/2}, \quad a = (h/g)^{1/2} \cdot \omega, \quad b = \frac{V}{(gh)^{1/2}}, \quad c = \frac{T}{gh^2},$$

$$\alpha = \frac{\varepsilon}{h}, \quad q(\lambda) = \frac{h}{\sqrt{2\pi}} \int_{-\infty}^{\infty} f(hx)\, e^{-i\lambda x}\, dx, \quad T = \frac{T'}{\rho}.$$

3. Steady-State Solution

We shall determine the asymptotic values of the integrals for large time at a large distance from the pressure segment.

The asymptotic values appear as contributions in the form of residues at the real poles of the integrands of the integrals in (2.6). These poles are the solutions of the following three equations, called the frequency equations :

$$\sigma - b\lambda - a = 0 \qquad \ldots (3.1)$$

$$\sigma - b\lambda + a = 0 \qquad \ldots (3.2)$$

$$\sigma + b\lambda - a = 0. \qquad \ldots (3.3)$$

We shall determine these roots for given values of the parameters a, b, c and α. The roots will be determined as the points of intersection of the frequency curve $m = \sigma$ and the straight lines $m = b\lambda + a$, $m = b\lambda - a$ and $m = -b\lambda + a$. Since the determination of the roots crucially depends upon the shape of the curve $m = \sigma$, so we turn our attention into the investigation of the shape of the curve. Its shape depends upon the parameters c and α. For $\alpha = 0$ and $c \neq 0$, the case described by Pramanik and Majumdar[1] there are two branches in the curve when $c < 1/3$, one

branch passing through origin is called the gravity branch and the other called capillary branch and for $c \geq 1/3$ there is only one branch, the capillary branch. Assuming that due to the existence of the parameter α there will be no abrupt change in the shape of the frequency curve we anticipate that in the case $\alpha \neq 0$, $c \neq 0$, the same two shapes shown in Figs. 1 and 2 are valid with, of course, different values of c separating the two cases. These two shapes are similar as the previous case excepting the capillary branch in which the gradient is finite when $\lambda \to \infty$.

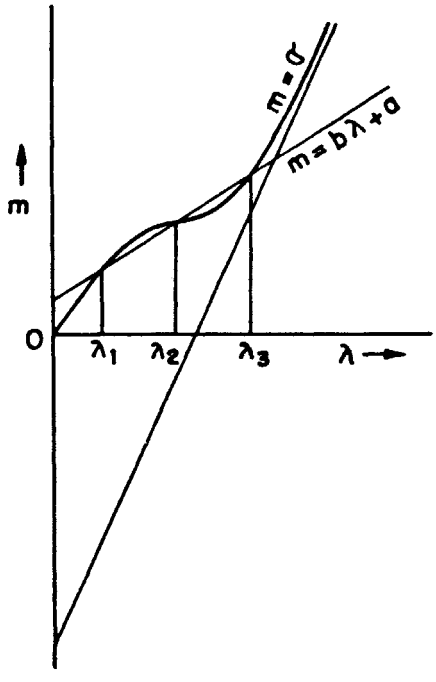

FIG. 1. The roots of eqn. (3.1) for $0 < c < ((1/3) + \alpha)$.

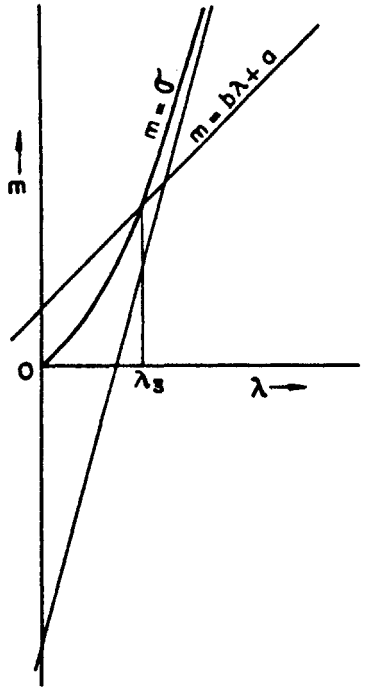

FIG. 2. The roots of eqn. (3.1) for $c \geq ((1/3) + \alpha)$.

There will be different ranges of values of (α, c) for which one of the two shapes will be appropriate. To determine these ranges we proceed as follows : we see that the gradients change differently in two shapes. In the shape in Fig. 1 gradient firstly decreases and then increases while in the other shape gradient gradually increases with increasing λ. To motivate this idea we consider the tangency of any line $m = b\lambda$ with $m = \sigma$. The condition of tangency is mathematically expressed as

$$\left.\begin{aligned} \sigma &= b\lambda \\ \sigma' &= b \end{aligned}\right\} \quad \text{for } 0 \leq \lambda < \infty. \qquad \ldots (3.4)$$

From this c can be expressed as a function of λ and α i.e.,

$$c = \frac{\tanh \lambda + 2\alpha\lambda \tanh^2 \lambda - \lambda \operatorname{sech}^2 \lambda}{\lambda^2 (\lambda \operatorname{sech}^2 \lambda + \tanh \lambda)} \quad \text{for} \quad 0 \leq \lambda < \infty. \qquad \ldots (3.5)$$

One can show with a little manipulation that $\frac{dc}{d\lambda} < 0$ for all values of α. Consequently for all values of α the curve (3.5) is monotonically decreasing with increasing λ and hence the maximum value of c occurs at $\lambda = 0$ and thus the maximum value is $((1/3)+\alpha)$. The shape of the curve (3.5) is shown in Fig. 3. It follows that for any $c < ((1/3)+\alpha)$ there is a value of λ for which the line $m = b\lambda$ is tangent to the curve $m = \sigma$ and hence Fig. 1 is appropriate. On the other hand for any $c \geq ((1/3)+\alpha)$ the line $m = b\lambda$ is never tangent to $m = \sigma$, so Fig. 2 is appropriate.

3.1. *Steady Waves for* $0 < c < ((1/3)+\alpha)$

In this case it is easy to show that the frequency curve $m = \sigma$ has a point of inflexion at some point $\lambda = \lambda_0$ (> 0) satisfying the following equation :

$$4[(1+\alpha\lambda\tanh\lambda)\,3c\lambda\tanh\lambda + (1+3c\lambda^2+2\alpha c\lambda^3\tanh\lambda)\,\mathrm{sech}^2\lambda$$

$$-(\lambda+c\lambda^3)\,\mathrm{sech}^2\lambda\tanh\lambda](1+\alpha\lambda\tanh\lambda)(\lambda+c\lambda^3)\tanh\lambda$$

$$-[(1+3c\lambda^2+2\alpha c\lambda^3\tanh\lambda)\tanh\lambda + (\lambda+c\lambda^3)\,\mathrm{sech}^2\lambda]$$

$$\times [3\alpha(\lambda\,\mathrm{sech}^2\lambda+\tanh\lambda)(\lambda+c\lambda^3)\tanh\lambda + (1+\alpha\lambda\tanh\lambda)$$

$$\times \{(\lambda+c\lambda^3)\,\mathrm{sech}^2\lambda + (1+3c\lambda^2)\tanh\lambda\}] = 0. \qquad \ldots (3.6)$$

It can be seen from Fig. 1 that eqn. (3.1) has, in general, three real positive roots $\lambda_1, \lambda_2, \lambda_3$, say $(\lambda_1 < \lambda_2 < \lambda_3)$, eqn. (3.2) has two such roots λ_4, λ_5, say

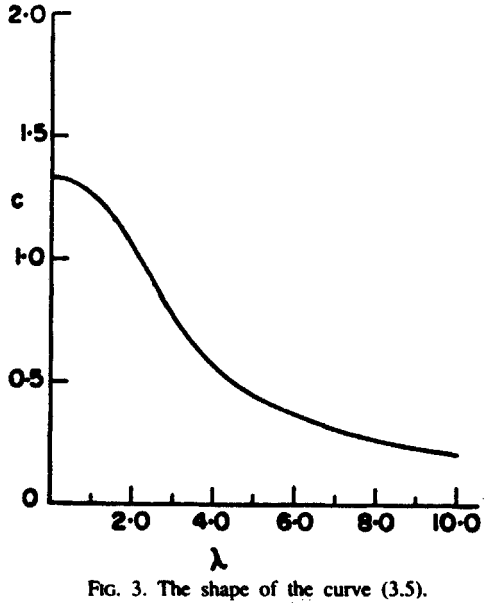

FIG. 3. The shape of the curve (3.5).

($\lambda_4 < \lambda_5$) and eqn. (3.3) has always one such root λ_6. The existence of the roots depends upon the values of the parameters a, b, c. This distribution can be known by a study of the cases where some of the roots coalesce, called the critical cases. Following Pramanik and Majumdar[1] the critical cases have the following representation

$$b = \frac{(1 + 3c\lambda^2 + 2\alpha c\lambda^3 \tanh\lambda)\tanh\lambda + (\lambda + c\lambda^3)\operatorname{sech}^2\lambda}{2(1 + \alpha\lambda\tanh\lambda)^{3/2}[(\lambda + c\lambda^3)\tanh\lambda]^{1/2}} \quad \text{for} \quad 0 \le \lambda < \infty \quad \ldots (3.7)$$

$$\left.\begin{aligned} a &= \frac{(\lambda - c\lambda^3 + 2\alpha\lambda^2\tanh\lambda)\tanh\lambda - \lambda(\lambda + c\lambda^3)\operatorname{sech}^2\lambda}{2(1 + \alpha\lambda\tanh\lambda)^{3/2}[(\lambda + c\lambda^3)\tanh\lambda]^{1/2}} \quad \text{for} \quad 0 \le \lambda < \lambda' \\ &= \frac{\lambda(\lambda + c\lambda^3)\operatorname{sech}^2\lambda - (\lambda - c\lambda^3 + 2\alpha\lambda^2\tanh\lambda)\tanh\lambda}{2(1 + \alpha\lambda\tanh\lambda)^{3/2}[(\lambda + c\lambda^3)\tanh\lambda]^{1/2}} \quad \text{for} \quad \lambda' \le \lambda < \infty \end{aligned}\right\} \quad \ldots (3.8)$$

where λ' is the value of λ for which the straight line $m = b\lambda$ is a tangent to the curve $m = \sigma$ and this value is given by

$$(1 - c\lambda^2 + 2\alpha\lambda\tanh\lambda)\tanh\lambda - (1 + c\lambda^2)\lambda\operatorname{sech}^2\lambda = 0. \quad \ldots (3.9)$$

Now for a fixed value of α eqns. (3.7) and (3.8) represent, in the parametric form a surface called the critical surface $f(a, b, c) = 0$ in the space of the parameters a, b, c. The intersecting curve of this surface by the plane c = constant can be drawn for certain values of c. For $\alpha = 0.1$ and $c = 0.07$ such a curve is shown in Fig. 4 where the point A_0 corresponds to $\lambda = \lambda_0$ and the point A' to $\lambda = \lambda'$. This curve starts from some finite point A and ends at the finite point B having co-ordinate $a = \frac{1}{2}(c/\alpha^3)^{1/2}$, $b = (c/\alpha)^{1/2}$. The curvilinear portions C_1, C_2 and C_3, extending respectively from the point A to A_0, from A_0 to A' and from A' to B represent the cases $\lambda_1 = \lambda_2$, $\lambda_2 = \lambda_3$ and $\lambda_4 = \lambda_5$ respectively. The straight lines DB, CB passing through the point B and parallel to the axes a, b as shown in Fig. 4 correspond to the values $a = \frac{1}{2}(c/\alpha^3)^{1/2}$, $b = (c/\alpha)^{1/2}$ respectively. Now the curves C_1, C_2, C_3 and the straight lines CB, DB divide in the whole positive quadrant of the plane (a – b) into 9 regions R_n (n = 1 to 9) as shown in Fig. 4 of which seven regions are distinct.

In each of those regions there corresponds a definite subset of the roots λ_r (r = 1 to 6) in the sense that the values of the parameters a, b which determine the region also fix the roots. The roots of eqns. (3.1), (3.2) and (3.3) can now be determined for all values of the parameters a, b. This can be achieved geometrically by considering Fig. 1 and Fig. 4 side by side. This procedure is explained in Pramanik and Majumdar[1]. So in the following we write down the distributions of these roots in various regions :

R_1	R_2	R_3	R_4	R_5	R_6	R_7	R_8	R_9
λ_1	λ_1, λ_2	$\lambda_1, \lambda_2, \lambda_3$	λ_3, λ_4	λ_3	λ_3	λ_4	λ_4	λ_1, λ_2
λ_6	λ_3, λ_6	$\lambda_4, \lambda_5, \lambda_6$	λ_5, λ_6	λ_6	λ_6	λ_6	λ_6	λ_4, λ_6

It is noted that the roots in the regions R_5 and R_6 and also in the regions R_7, R_8 are identical. For points (a, b) on the critical curve the roots can also be similarly determined. It is to be noted that for each point on the critical curve, two of the roots coincide excepting the point A_0 where three roots coincide.

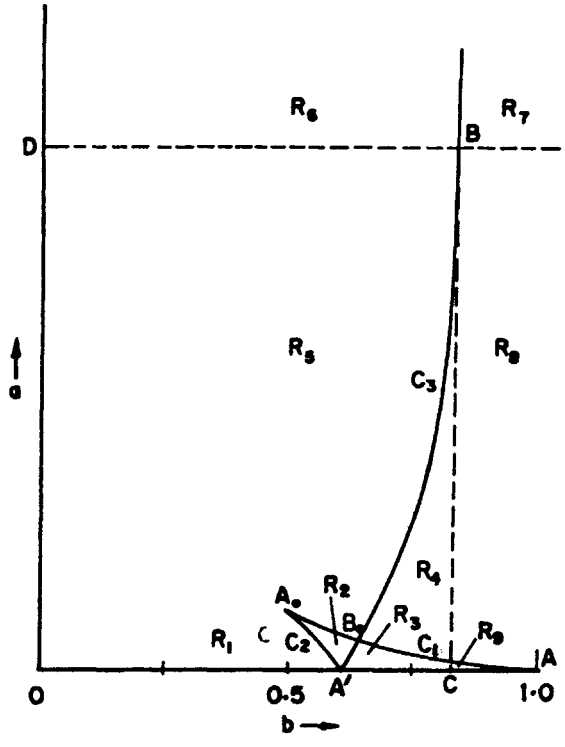

FIG. 4. The section of the critical surface in the $(a - b)$ plane for $c = 0.07$, $\alpha = 0.1$.

We are now in a position to determine the asymptotic waves at far field after a large time. These asymptotic waves come as contributions to the asymptotic values of the integrals in terms of the poles of the integrands in (2.6). In the following we firstly write down the waves for (a, b) in the region R_3 where all the waves η_r $(r = 1$ to $6)$ exist

$$\left.\begin{aligned} \eta &= \eta_1 + \eta_3 + \eta_5 \quad \text{as} \quad t \to \infty, \ x \to \infty \\ &= \eta_2 + \eta_4 + \eta_6 \quad \text{as} \quad t \to \infty, \ x \to \infty \end{aligned}\right\} \qquad \ldots (3.10)$$

where

$$\eta_1 = H_1(\lambda_1)\exp\{i(at-\lambda_1 x)\}, \qquad \eta_2 = -H_1(\lambda_2)\exp\{i(at-\lambda_2 x)\},$$

$$\eta_3 = H_1(\lambda_3)\exp\{i(at-\lambda_3 x)\}, \qquad \eta_4 = H_2(\lambda_4)\exp\{i(at+\lambda_4 x)\},$$

$$\eta_5 = -H_2(\lambda_5)\exp\{i(at+\lambda_5 x)\}, \qquad \eta_6 = H_3(\lambda_6)\exp\{i(at+\lambda_6 x)\}$$

and

$$H_1(\lambda) = \frac{\pi i}{2\rho g h (2\pi)^{1/2}} \cdot \frac{\lambda q(-\lambda)\tanh\lambda}{(1+\alpha\lambda\tanh\lambda)[\sigma'(\lambda)-b]\sigma(\lambda)}$$

$$H_2(\lambda) = \frac{\pi i}{2\rho g h (2\pi)^{1/2}} \cdot \frac{\lambda q(\lambda)\tanh\lambda}{(1+\alpha\lambda\tanh\lambda)[\sigma'(\lambda)-b]\sigma(\lambda)}$$

$$H_3(\lambda) = \frac{\pi i}{2\rho g h (2\pi)^{1/2}} \cdot \frac{\lambda q(\lambda)\tanh\lambda}{(1+\alpha\lambda\tanh\lambda)[\sigma'(\lambda)+b]\sigma(\lambda)}.$$

The wave system for the case when the values of the parameters a, b are such that the point (a, b) lies in other regions is easy to determine. This is the same wave-system as expressed in (3.10), only the wave corresponding to a pole not occurring in a region being deleted for that region. Thus we see that for the points (a, b) in R_3 the steady state consists of six progressive waves. Among these, the waves $\eta_1, \eta_2, \eta_4, \eta_6$ are the gravity waves and the rest are the capillary waves. Three gravity waves exist in the downstream side and one in the upstream side, while both the capillary waves exist in the upstream side.

3.2. *Steady Waves for* $c \geq \left(\frac{1}{3}+\alpha\right)$

It is evident from Fig. 2 that the roots of the frequency equations in the present case are $\lambda_3, \lambda_4, \lambda_5, \lambda_6$. And λ_4, λ_5 may coincide to give rise to the critical case which is represented as follows :

$$\left.\begin{aligned} a &= \frac{\lambda(\lambda+c\lambda^3)\operatorname{sech}^2\lambda - (\lambda - c\lambda^3 + 2\alpha\lambda^2\tanh\lambda)\tanh\lambda}{2(1+\alpha\lambda\tanh\lambda)^{3/2}[(\lambda+c\lambda^3)\tanh\lambda]^{1/2}} \\ b &= \frac{(1+3c\lambda^2+2\alpha c\lambda^3\tanh\lambda)\tanh\lambda + (1+c\lambda^3)\operatorname{sech}^2\lambda}{2(1+\alpha\lambda\tanh\lambda)^{3/2}[(\lambda+c\lambda^3)\tanh\lambda]^{1/2}} \end{aligned}\right\} 0 < \lambda < \infty$$

... (3.11)

The intersecting curve C_4 of the critical surface (3.11) is drawn for $c = 1$ and $\alpha = 0.4$ in Fig. 5. This curve starts from E and ends at some finite point F and it represents the case $\lambda_4 = \lambda_5$. The straight lines FH and FG passing through the point F and parallel to the axes a, b as shown in Fig. 5 correspond to the values

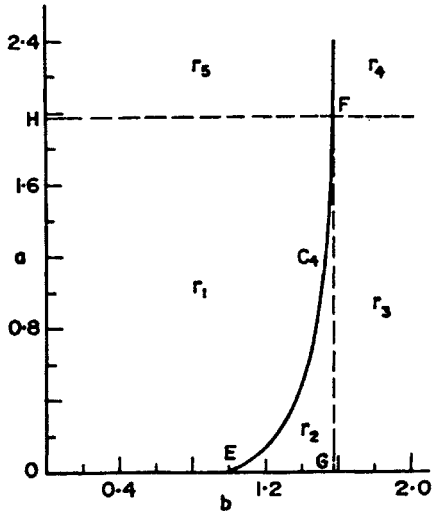

FIG. 5. The section of the critical surface in the $(a - b)$ plane for $c = 1$, $\alpha = 0.4$.

$a = \frac{1}{2}\left(\frac{c}{\alpha^3}\right)^{1/2}$, $b = \left(\frac{c}{\alpha}\right)^{1/2}$ respectively. The curve C_4 and these straight lines divide the whole positive quadrant of the $(a - b)$ plane into five regions r_n (n = 1 to 5) as shown in Fig. 5 of which 3 regions are distinct. As before we write down the distribution of the roots $\lambda_3, \lambda_4, \lambda_5, \lambda_6$ in the regions :

r_1	r_2	r_3	r_4	r_5
λ_3	λ_3, λ_4	λ_4	λ_4	λ_3
λ_6	λ_5, λ_6	λ_6	λ_6	λ_6

As the case $c < \left(\frac{1}{3} + \alpha\right)$, the steady-state value of η in each region can be calculated. Here only we write down the same in region r_2 for the points (a, b) of which all the waves $\eta_3, \eta_4, \eta_5, \eta_6$ exist

$$\eta = \eta_3 + \eta_5 \quad \text{as} \quad t \to \infty, \; x \to \infty$$

$$= \eta_4 + \eta_6 \quad \text{as} \quad t \to \infty, \; x \to -\infty$$

The comparison of the present results with those in the non-inertial case reveals the effect of inertial surface on the resulting waves. It is seen that for both the ranges $0 < c < \left(\frac{1}{3} + \alpha\right)$ and $c \geq \left(\frac{1}{3} + \alpha\right)$ the intersecting curve dividing the whole positive quadrant of the $(a - b)$ plane into several regions is different here. Each of the curves C_1, C_2, C_3 and C_4 are somewhat shortened in the present case. This shortening

is more apparent for the curves C_3 and C_4. The curves C_3, C_4 in the non-inertial case go upto infinity but here they are terminated at finite points. As a result of such change the existence of the waves for different values of (a, b) is altered from that in the non-inertial case and it can be easily verified that existence of the waves are restricted in the present case. This means that a particular wave that exists in non-inertial case for certain values of (a, b) may not exist in the present case for the same values of (a, b). As an illustration we consider the region R_3. It is easy to verify that the set of points (a, b) comprising the region R_3 is smaller in the present case than the corresponding set in the previous case. As a result the cases of existence of all the gravity and capillary waves are much restricted than the previous case. Also consideration of waves above the line DB and to the right of CB establishes the fact more clearly. For the points (a, b) in R_7, both the capillary waves η_3 and η_5 do not exist in the present case but in the non-inertial they exist in the corresponding region. The similar phenomenon occurs for the points (a, b) in the region R_4. The restriction of the inertial surface on the propagation of waves is more apparent on the capillary waves η_3 and η_5. In the non-inertial case either both wave present or both absent. But in the present case, the region where both are present is again subdivided into two in one of which only one wave is present. Thus it follows that the inertial surface can prohibit the propagation of capillary waves more effectively than that of the gravity waves.

The physical reason is, of course, clear. The capillary waves are of short wave length. So it is obvious that they are easily damped out by the inertial surface.

ACKNOWLEDGEMENT

The authors wish to thank the referee for some suggestions of improvements.

REFERENCES

1. A. K. Pramanik, S. R. Majumdar, *J. Fluid Mech.* **145** (1984), 405-15.
2. A. B. Peters, *Comm. Pure Appl. Math.* **3** (1950), 319-54.
3. P. F. Rhodes-Robinson, *J. Austral. Math. Soc. Ser. B* **25**, (1984), 366-83.